Available online at www.sciencedirect.com
ScienceDirect
Ceramics International 36 (2010) 2103–2115
CERAMICS INTERNATIONAL
www.elsevier.com/locate/ceramint

Ballistic performance of armour ceramics: Influence of design and structure. Part 1

Eugene Medvedovski *

Umicore Indium Products, 50 Sims Ave., Providence, RI 02909, USA

Received 28 August 2009; received in revised form 23 February 2010; accepted 2 May 2010
Available online 23 June 2010

Abstract

The use of advanced ceramics for armour systems allows the defeating of the projectile and ballistic impact energy dissipation providing adequate ballistic protection. The development of lightweight and inexpensive ceramics and armour designs is under ongoing attention by both ceramic armour manufacturers and armour users. This paper summarizes the results of extensive studies of ballistic performance of different armour ceramics, mostly obtained during development, as well as of the materials manufactured by other recognized armour ceramic suppliers, and the designed ceramic-based armour systems. The studied armour ceramics include homogeneous oxide and carbide ceramics and heterogeneous ceramic materials. Composition, structure and main properties of the considered ceramics, which affect ballistic performance, are examined and analyzed. Only a combination of all relevant physical properties and microstructure, including the ability to dissipate ballistic energy, as well as optimization of manufacturing processes, should be considered for proper selection and evaluation of ceramic armour. Ballistic performance of the studied ceramics as function of their structure and properties, armour system design and type of projectile has been discussed.

Keywords: B. Composites; B. Microstructure-final; E. Armour; Ballistic performance

1. Introduction

During the last decade, intensive studies were devoted to the development of lightweight armour systems for personnel, vehicle, helicopter and structural applications and their ballistic performance. Advanced ceramics is one of the most important components of modern armour systems. As a component of the armour systems, advanced ceramics assist to defeat projectiles through the ballistic impact energy dissipation. The mechanisms of ballistic protection for ceramic and metal armour are significantly different. While metallic armour absorbs the energy of projectile by a plastic deformation mechanism, in the case of ceramics, the kinetic energy of the projectile is dissipated through fracture. Usually ceramic armour systems consist of a monolithic ceramic or composite ceramic-metal body covered by ballistic nylon and bonded with a high tensile strength fiber lining or laminated polyethylene, such as Kevlar™, Twaron™, Spectra™, Dyneema™, placed on the back of the ceramic or ceramic–metal composite. Some soft metals (e.g. aluminum thin sheets) may be also used as a backing material. In some cases, a spall shield is attached on the front of armour. Upon impact of the bullet (velocity greater than 700–1000 m s^{-1}), the hard ceramic body used is cracked and broken, and the residual energy is absorbed by the soft reinforced backing material. This backing material must support the post-impact fracturing of the ceramic body and the defeated bullet. Soft covering of the armour also protects the system against possible damage associated with vibrations.

Different ceramic materials are commonly used for ballistic protection; they include some oxide ceramics (mostly, alumina ceramics with different contents of Al_2O_3) and non-oxide ceramics (mostly carbides, nitrides, borides and their combinations) [1–11]. Despite elevated density (up to 3.95 g cm^{-3}), alumina ceramics are widely used for ballistic protection as they provide relatively high physical properties and performance, low cost and an ability to be manufactured using a variety of methods, e.g. slip casting, pressing, injection moulding, without the use of expensive equipment, such as kilns with special protective atmospheres. Recently developed

---

* Tel.: +1 401 215 1704/480 1905; fax: +1 401 421 2419.
E-mail addresses: emedvedovski@cox.net, emedvedovski@shaw.ca, Eugene.Medvedovski@am.umicore.com.

0272-8842/$36.00 © 2010 Elsevier Ltd and Techna Group S.r.l. All rights reserved.
doi:10.1016/j.ceramint.2010.05.021

alumina–mullite ceramics with lower density provide weight reduction accordingly, and these materials also are inexpensive and have a good manufacturing ability [12]. In comparison, non-oxide dense ceramics, e.g. boron carbide (B_4C), silicon carbide (SiC), silicon nitride (Si_3N_4), aluminum nitride (AlN) and some others (excepting titanium diboride-based ceramics), including the materials based on their binary systems (e.g. B_4C–SiC, SiC–Si_3N_4), have low densities in the range of 2.5–3.3 g cm^{-3} (important for ballistic protection systems). These materials have high mechanical properties, e.g. hardness, Young's modulus, strength. However, in many cases, these ceramics are manufactured by hot pressing that is expensive and not very productive. Although pressureless sintered materials, such as commercially produced SiC ceramics, may be less expensive than hot-pressed, they are still relatively expensive because their manufacturing requires kilns with special controlled atmospheres and very high temperatures for sintering. Reaction-bonded silicon carbide (RBSC) and boron carbide (RBBC) and some other reaction-bonded carbide-based ceramics are also extensively used for armour applications due to their relatively lower cost, high physical properties and an ability to manufacture relatively large-sized products [13,14]. These reaction-bonded materials also demonstrate better integrity for multi-hit situations than dense homogeneous carbide-based ceramics.

Ceramic-matrix composites, which may consist of whiskers, fibres, particulates reinforcing the ceramic ingredient, or a metallic phase (such as Al, Ni and some others) introduced by the infiltration routes, also demonstrate a high integrity after ballistic impact due to their mechanical properties and impact energy dissipation ability [4]. Metal-infiltrated composites, e.g. such as B_4C/Al [2], Lanxide^{TM} SiC/Al (which were produced some time ago) and some others, with a high integrity to ballistic impact are not widely used for ballistic protection due to high cost of their processing and equipment, and they may be prone to problems in manufacturing. Also these materials can be employed only against low-hardness mild steel projectiles (they cannot withstand hard steel and, moreover, WC threats), especially if these composites contain a rather high amount of bonding soft metallic phase. It should be noted that the majority of starting materials for ceramic-matrix composites, as well as for non-oxide armour ceramics, are rather expensive, that additionally increases the cost of such armour.

This paper summarizes the results of the extensive studies of ballistic performance of different armour ceramics, mostly obtained during development and manufacturing, as well as materials obtained from other recognized armour ceramic suppliers, and the designed ceramic-based armour systems. The studies results of the majority of armour ceramics, excepting silicon nitride-based and SiAlON ceramics, which also may have a great potential due to their light density and high mechanical properties, including high fracture toughness, are reported here (transparent armour ceramics were not also included to the current study). It should be mentioned that the majority of armour materials, which were obtained through development and manufacturing, such as alumina and alumina–mullite ceramics, heterogeneous silicon carbide-based ceramics (e.g. AS and ASN grades), are not expensive, their manufacturing is efficient, and it does not require expensive equipment, such as hot presses or high-temperature furnaces with controlled atmosphere, which are generally not very productive. Ballistic performance of the armour ceramics and systems was evaluated by actual shooting using military weapon and variety of ammunition.

2. Experimental

The studied armour ceramic materials include dense homogeneous high-alumina ceramics with Al_2O_3 contents ranging 97–99.7 wt.% (denoted as AL), alumina–mullite ceramics based on optimized ratios of Al_2O_3 and mullite with selected sintering aids (denoted as AM) and based on the starting system of alumina and zircon yielding alumina, mullite and ZrO_2 (denoted as ZAS), dense homogeneous silicon carbide and boron carbide ceramics, reaction-bonded silicon carbide and boron carbide ceramics (RBSC and RBBS), including biomorphic reaction-bonded silicon carbide, with heterogeneous structures, and heterogeneous silicon carbide-based ceramics obtained based on the systems SiC–Al_2O_3, SiC–Si_3N_4–Al_2O_3, SiC–Si_3N_4–SiAlON (denoted as AS, ASN, ESS and ESAS, respectively). Manufacturing of the developed alumina and alumina–mullite ceramics was described earlier [8,12]. Dense silicon carbide and boron carbide ceramics were produced by hot pressing and by pressureless sintering (mostly, by liquid phase sintering) technology. Most of them were received from recognized armour ceramic suppliers; however, some tested pressureless sintered carbide compositions have been prepared jointly with other organizations. RBSC and RBBC ceramics were also obtained from the recognized armour ceramic suppliers, and their technology is based on molten silicon infiltration of SiC or B_4C preforms; biomorphic RBSC ceramics were processed via silicon infiltration of the wooden preforms carbonized by high-temperature pyrolysis [15]. Manufacturing of the developed heterogeneous SiC-based ceramics AS, ASN, ESS, ESAS was described earlier [14]. The armour systems were prepared using commercially available backing materials based on the proposed designs. The system designs, including material selection and thickness, were elaborated depending on the performance requirements and actual thickness of front armour ceramics. Bonding of the backing was conducted in autoclave using a commercial established procedure. As backing materials, well known aramid-based fabric materials of different grades (e.g. Kevlar^{TM}, Twaron^{TM}) and polyethylene (e.g. Spectra^{TM}) were used. Fiberglass layer or wrapping of ceramic armour components was applied at the bonding stage.

Ceramic phase composition and structure were studied using XRD and SEM analyses, respectively. Physical properties, which are relevant to ballistic performance, of the ceramic samples cut from actual armour ceramic articles were determined in accordance with the methods and procedures related to the standards used for advanced ceramics. Special attention was paid to hardness measuring due to a large variance in the data and interpretation of the results reported in different

Table 1
Ammunition used in ballistic performance testing.

Ammunition	Description	Weight, g	Velocity, g cm^{-3}	Energy, kJ
5.56 × 45 mm SS109	NATO Ball FMJ steel tip ball	4	930–1000	1.73–2.0
7.62 × 39 mm	Russian Ball FMJ mild steel core	8	710–740	2.02–2.19
7.62 × 51 mm	NATO Ball FMJ lead core	9.65	854	3.52
0.308 Win	Winchester 7.62 × 51 mm Ball FMJ	9.7	838–859	3.41–3.58
7.62 × 54R LPS	Russian Ball LPS streamlined ball steel core	12	818	4.01
0.308 Lapua	Lapua 7.62 × 51 mm Ball FMJ	11	860	4.07
7.62 × 63 mm AP M2	Armour piercing M2 FMJ WC core	10.8	830–868	3.72–4.07

sources. The detailed sample preparation and hardness measuring procedure were reported earlier [16]. Indentation replicas were also observed in an optical microscope to determine the presence of crack propagation. Fracture toughness was calculated from the Vickers indentation. Brittleness (*B*) of homogeneous ceramic materials was calculated using a formula [17]:

$$B = \frac{HV \cdot E}{K_{Ic}^2}$$

where HV is Vickers hardness, E is Young's modulus, and K_{Ic} is fracture toughness.

Ballistic energy dissipation ability (*D*-criterion) for the studied ceramics was calculated in accordance with the formula proposed by Neshpor et al. [8]:

$$D = \frac{0.36(HV \cdot E \cdot c)}{K_{Ic}^2}$$

where c is sonic velocity.

Ballistic performance of the ceramics bonded with appropriate backing materials was tested in the Ceramic Protection Corporation (Calgary, AB, Canada) shooting range in accordance with the NIJ 0101.03 and NIJ 0101.04 standards using the weapon M16. Depending on the application and the required level of protection, the military ammunitions, such as 5.56 × 45 SS109 with a steel tip ball, 7.62 × 51 mm NATO Ball Full Metal Jacket (FMJ) with a lead core, 7.62 × 39 mm Russian Ball FMJ with a steel core, 7.62 × 54R Russian Ball LPS, 7.62 × 63 mm Armour Piercing M2 FMJ with a tungsten carbide core, 0.308 Win and 0.308 Lapua, were used. Depending on the ammunition, the bullet weight, velocity and energy have different values (Table 1). The study of ballistic performance using actual military ammunition is important because fragmentation of the ceramics depends on actual conditions, and it distinguishes from modeling conditions when "artificial" projectiles are applied. The projectile velocity was controlled using a chronograph. The trauma after shooting was evaluated using a Roma Plastilina modeling clay placed behind the armour system; the trauma in clay duplicated the transient deformation of the composite armour on the back of the system. The damage zone of the ceramics, including ceramic fragmentation, and the subsequent post-impact condition of bullets after shooting were observed. Flat tiles with sizes of 100 × 100 mm × (7–10) mm and 155 × 200 mm × (7–10) mm, as well as actual armour plates and panels of different configurations and thicknesses of 4–10 mm, were ballistically tested; actual armour articles were used for multi-hit testing (with approximately 50 mm spacing between hits).

3. Results and discussion

3.1. Microstructure and phase composition of studied armour ceramics

Phase composition and microstructure of dense alumina ceramics AL97ML, AL98 and AL98.5 ceramics (the figures denote approximate Al_2O_3 contents) are similar, and they consist of corundum grains, as the major phase, bonded by a small amount of anorthite crystals and a silicate-based glassy phase. A small amount of mullite grains is also present in the AL97ML ceramics. The AL99.7 ceramics consists of corundum grains bonded by tiny grains of spinel and a very small amount of a glassy phase formed due to the presence of oxide-impurities. Generally, the structure of the studied alumina ceramics is uniform and microcrystalline (Fig. 1a–d). The grain size of the alumina ceramics depends on the initial batch composition, initial particle size and particle size distribution of starting alumina powders. Alumina powders with a smaller particle and median crystal size provide a fine-crystalline structure with a smaller grain size. The average corundum grains range from 1 to 3 μm for the AL99.7 (mostly isometric) to 3–6 μm (isometric) and (2–3) μm × (5–10) μm (short prismatic) for the AL97ML ceramics. A glassy phase is distributed uniformly between grains and, as expected, the amount of the glassy phase increases as the alumina content decreases. Opposite to alumina ceramics, even AL99.7 with the highest content of a crystalline phase, alumina–zirconia ceramics AZ practically does not have a glassy phase; the zirconia phase (about 0.5 μm grain size) is very uniformly distributed among alumina grains with sizes of 1–1.5 μm (Fig. 1d).

Alumina–mullite ceramics (AM materials) also have a dense homogeneous fine-grained microstructure (Fig. 2) formed by corundum grains (a major phase) with uniformly distributed mullite grains cemented by an aluminosilicate glassy phase. The grain size of these ceramics is 2–4 μm (mostly isometric) with a presence of larger grains (up to 6 μm); smaller grains with a size of 0.5–1 μm are also noted. The optimized AM2 composition has a relatively low content of a glassy phase. A

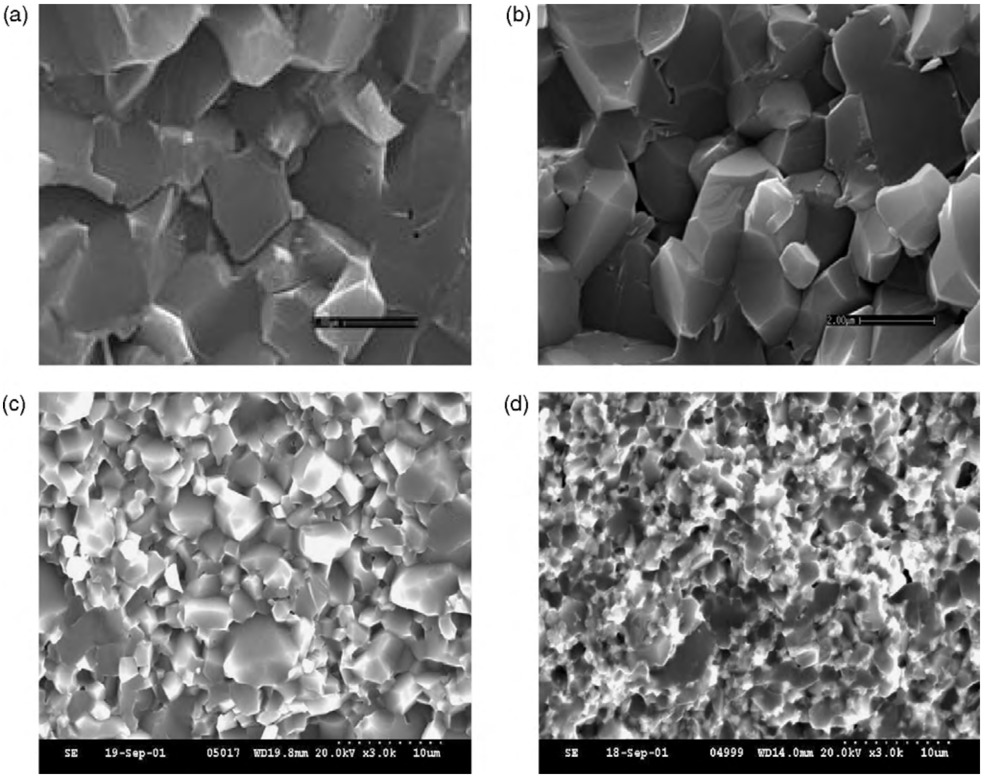

Fig. 1. Microstructure of alumina ceramics. (a) AL98; (b) AL98.5; (c) AL99.7; (d) AZ.

reduction of density of alumina–mullite ceramics is exhibited to 3.5–3.56 g cm^{-3} vs. 3.75–3.91 g cm^{-3} for alumina ceramics. Alumina–mullite ceramics with additional zircon and zirconia phases (ZAS materials) also have microcrystalline structures but density of these ceramics is slightly greater (3.6–3.75 g cm^{-3}, depending on compositions). ZAS ceramics with higher contents of zircon in the batch composition have higher contents of a glassy phase and lower density.

Homogeneous B_4C and SiC armour ceramics have very uniform microcrystalline structures (several microns average grain size) without foreign phases. Hot-pressed ceramics have a denser structure with minimal porosity and higher density values (up to 98–99% of TD) but larger grain sizes (up to 10–15 μm). A grain boundary oxide glassy phase is present if oxide sintering aids are used for the SiC ceramic composition.

RBSC and RBBC ceramics manufactured by several ceramic producers are dense with low open porosity, and they have heterogeneous structures formed by SiC or B_4C grains of different sizes up to 50–100 μm (different manufacturers use starting carbide powders with different particle sizes) bonded by fine SiC grains (β-SiC) and residual silicon; the amount of the silicon phase is approximately 10–12% (Fig. 3a and b). Their structures depend on the size of starting SiC or B_4C materials and particle size distribution, on the source of carbon (mostly, type of organic binders and feature of their pyrolysis) and applied technology. Biomorphic RBSC consists of a lower content of SiC (mostly β-SiC formed due to interaction of Si with C) and a significantly higher content of residual Si (about 30 vol.% based on calculation) with a very small amount (up to 3 vol.%) of carbon. The structure of biomorphic RBSC

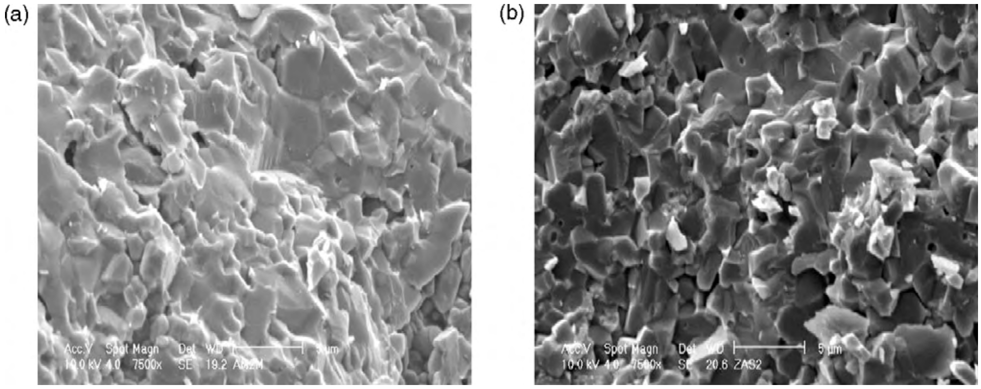

Fig. 2. Microstructure of alumina–mullite ceramics. (a) AM2; (b) ZAS2 (prepared in the system Al_2O_3–SiO_2–ZrO_2).

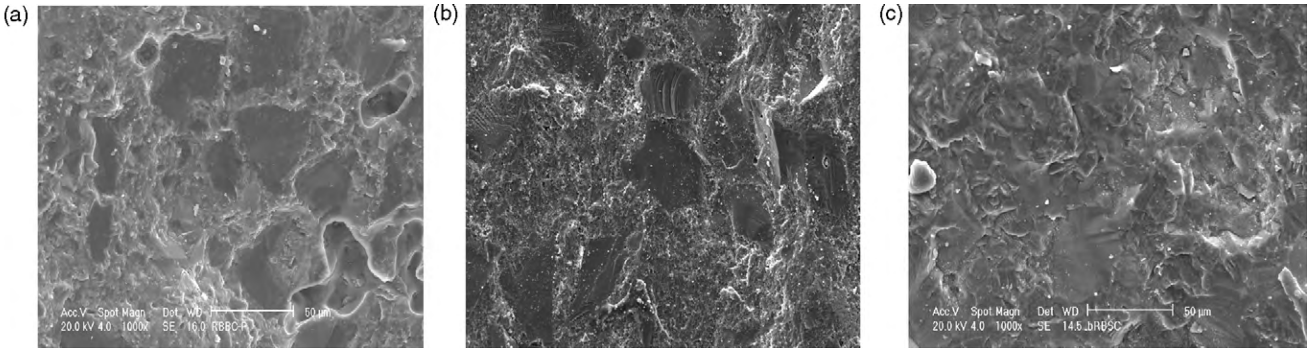

Fig. 3. Microstructure of reaction-bonded carbide ceramics. (a) RBBC; (b) RBSC; (c) biomorphic RBSC.

(Fig. 3c) is more homogeneous than ‘‘conventional’’ RBSC that is defined by the used wooden preform. The SiC grains have sizes of 5–20 μm, i.e. smaller than ‘‘conventional’’ RBSC. Due to a relatively high content of residual Si, density of this ceramic is lower than ‘‘conventional’’ RBSC (about 2.8 g cm^{-3} at water absorption of not greater than 0.02% vs. 2.98–3.07 g cm^{-3}, respectively).

The ceramics developed in the system of SiC–(Si_3N_4)–Al_2O_3 (AS and ASN materials) have a heterogeneous structure (Fig. 4a and b). It is formed by SiC grains with different sizes ranging from 3–5 to 120 μm bonded by a crystalline–glassy silicon carbide–aluminosilicate matrix. In the case of the use of Si_3N_4 constituent in the compositions (ASN materials), the bonding phase also includes silicon nitride and sialon. The compaction between SiC grains is rather high, and it is achieved by specially selected ratios between the sizes of starting SiC particles. A high level of bonding between grains and the matrix is achieved through a reaction-bonding mechanism. This reaction bonding occurs due to partial oxidation of some ingredients and the following high-temperature interaction of alumina with the products of the noted oxidation process. The structure in general and the bonding phase in particular are denser in the case of the nitride-based bonding phase. The use of small amounts of specially selected inorganic additives also promotes the liquid phase formation and the interaction between phases during firing. These ceramics have some porosity, but the pore size is small (approximately several microns), and the pores are uniformly distributed. The majority of initial pores between grains, which occur at the green body formation stage, may disappear during the firing process when the liquid phase is formed and the mullite crystals are initiated and grown. The surface of the ceramics has a higher content of a glassy phase than subsurface areas. This is a result of the firing conditions and the features of the physico-chemical processes, defined by the diffusion mechanism, which occur during firing.

The ceramics made in the starting component systems of SiC–Si, SiC–Al_2O_3–Si and SiC–Si_3N_4–Al_2O_3–Si (ESS and ESAS materials) also have heterogeneous structures with SiC grains ranging from 3–5 to 120 μm (Fig. 4c). The bonding phase is represented by silicon nitride and, in the case of the Al_2O_3-constituent, by SiAlON with a presence of a small amount of residual silicon. The bonding phases in these ceramics are formed due to reaction-bonding mechanisms occurred during nitridation. The ceramics also have small porosity with very fine pore sizes. The SiAlON-bonded silicon carbide ceramics (i.e. the ceramics based on the initial system of SiC–Si_3N_4–Al_2O_3–Si) have lower porosity than other materials from this group.

3.2. Physical properties of armour ceramics

Physical properties related to ballistic performance of the considered ceramics are performed in Tables 2–6. Properties of dense alumina and alumina–mullite ceramics depend on the Al_2O_3 content, the size and shape of corundum grains, the amount, composition and distribution of a glassy phase

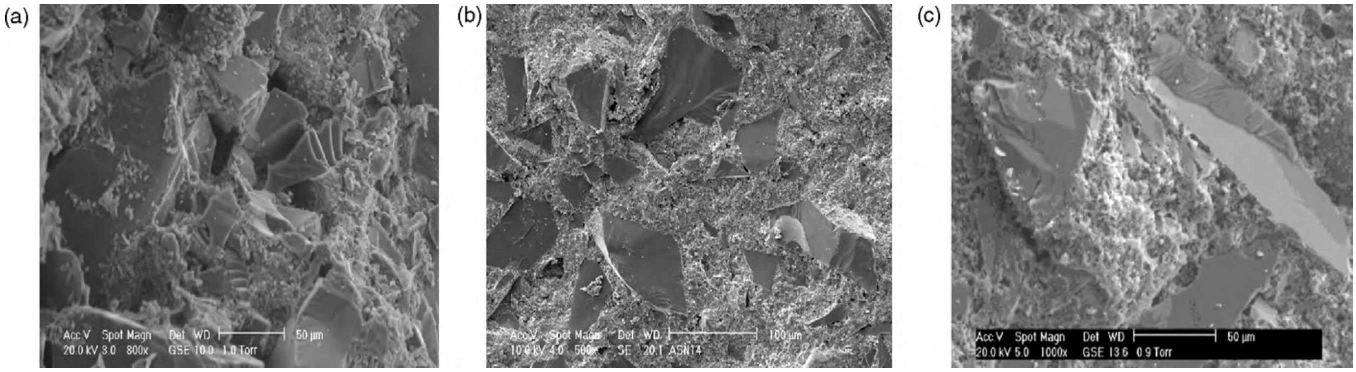

Fig. 4. Microstructure heterogeneous SiC–(Si_3N_4)–Al_2O_3 ceramics. (a) AS ceramics made from the starting system SiC–Al_2O_3; (b) ASN ceramics made from the starting system SiC–Si_3N_4–Al_2O_3; (c) ESAS ceramics made from the starting system SiC–Si_3N_4–Al_2O_3–Si.

Table 2
Properties of the studied alumina armour ceramics.

Property	AL97ML	AL98	AL98.5	AL99.7
Density[a], g cm^{-3}	3.74–3.76	3.78–3.82	3.81–3.84	3.90–3.91
Young's modulus, GPa	280–300	325–360	370–420	400–450
Sonic velocity, km s^{-1}	9.5–9.9	10.0–10.5	10.6–11.3	10.7–11.6
Vickers hardness *HV10*	1230–1260	1220–1330	1320–1420	1520–1560
Fracture toughness, K_{Ic}, MPa m$^{0.5}$	3.0–3.3	3.2–3.3	3.3–3.4	3.1–3.4
Flexural strength, MPa	–	250–350	270–360	320–380
Brittleness, $B \times 10^{-6}$, m^{-1}	340–380	370–430	420–460	525–545
Ballistic energy dissipation criterion, $D \times 10^{-12}$, s^{-1} (calculated)	1.70–1.95	1.50–1.60	1.80–1.95	2.20–2.40

[a] Water absorption is not greater than 0.02%.

cementing the crystalline phase, the presence and composition of the ''secondary'' phase, as well as the difference in thermal expansion between crystalline and glassy phases, and close porosity (i.e. sintered state) (Table 2). Properties also depend on the ''stressed'' conditions at the boundary of the corundum and the glassy phases, which are governed by the wetting of alumina particles with a liquid phase, interaction between the phases in sintering and by the firing conditions. A proper selection of alumina starting materials that allows optimizing ceramic microstructure with desirable grain sizes and physical properties is considered as one of the important factors of the ceramic improvement. Alumina ceramics with high corundum contents and a fine microstructure generally demonstrates higher values of mechanical properties, such as hardness, strength, Young's modulus and sonic velocity. Regarding alumina–mullite ceramics, an amount of the mullite phase or a ratio of corundum and mullite contents and glassy phase content define the properties of the ceramics in a sufficient extent. Although physical properties of alumina–mullite ceramics are not as high as high-alumina ceramics with the only major corundum phase and low contents of a glassy phase, both types of materials have comparable brittleness values or even lower than of the brittleness of the ceramic grades with higher Al_2O_3 contents (Table 3). Alumina–zirconia ceramics has superior properties comparatively with alumina ceramics and lower brittleness dealt with the presence of a zirconia phase, but, because of its elevated density (4.3–4.4 g cm^{-3}), its use is limited for armour application.

Similar factors, such as a content of the major phase, fine grain size and minimizing of close porosity, define high mechanical properties of dense homogeneous B_4C and SiC ceramics (Table 4). These ceramics have high-hardness values but only at the indentation loads below 1 kg. At higher loads, Vickers and Knoop hardness cannot be determined accurately due to shattering of the ceramics; dense carbide ceramics, particularly, B_4C-based ceramics, demonstrate a strong cleavage plane, especially at elevated loads. It is an obvious demonstration of high brittleness of this type of ceramics. As can be seen, hot-pressed materials demonstrated higher values of related properties than pressureless sintered materials due to a greater extent of densification. It has to be recognized that the properties data for pressureless sintered SiC ceramics reported in this paper are rather limited because only limited kinds of such ceramics were studied. Although some experimental ceramic compositions based on the systems B_4C–TiB_2–ZrB_2, B_4C–TiB_2, B_4C–$MoSi_2$ and B_4C–SiC obtained by pressureless sintering (in the framework with Alberta Research Council, Canada) had rather high density and hardness (HV0.3–HV1 greater than 2000 kg mm^{-2}), their properties were below than hot-pressed B_4C ceramics.

Properties of heterogeneous reaction-bonded ceramics, such as RBSC and RBBC and silicon carbide-based ASN, ESS, ESAS materials bonded with aluminosilicate, aluminosilicate–silicon nitride and aluminosilicate–sialon phases, are defined by the compaction and grain size distribution of the major SiC phase and quantity, distribution and composition of the bonding

Table 3
Properties of the studied alumina–mullite and alumina–zirconia ceramics.

Property	AM2	AM5	ZAS2	ZAS3	AZ
Density[a], g cm^{-3}	3.52–3.56	3.52–3.55	3.70–3.75	3.58–3.62	4.35–4.39
Vickers hardness *HV10*					
kg mm^{-2}	1130	1030	1180	940	1560
GPa	11.1	10.1	11.6	9.2	15.3
Rockwell hardness *HRA*	90.5	89	90	85	95
Fracture toughness, K_{Ic}, MPa m$^{0.5}$	2.54	2.32	3.03	3.08	4.0
Sonic velocity, km s^{-1}	8.62	8.76	9.04	8.38	9.9
Young's modulus, GPa	237	241	275	228	325
Flexural strength, MPa	350	300	350	275	530
Brittleness, $B \times 10^{-6}$, m^{-1}	408	452	347	221	300
Ballistic energy dissipation criterion, $D \times 10^{-12}$, s^{-1}	1.3	1.4	1.1	0.7	1.17

[a] Water absorption is not greater than 0.02%.

Table 4
Properties of the studied dense homogeneous carbide ceramics.

Property	B_4C hot-pressed	B_4C pressureless sintered	SiC pressureless sintered
Density[a], g cm^{-3}	2.5	2.4–2.45	3.06–3.10
Rockwell hardness *HRA*	94–95	93–94	90–92
Knoop hardness *HK1*			
kg mm^{-2}	2050–2250	1900–2100	1870–2020
GPa	20–22	18.5–20.5	18.3–20
Vickers hardness *HV1*			
kg mm^{-2}	2350–2450	2250–2400	2200–2300
GPa	23–24	22–23.5	21.5–22.5
Fracture toughness, K_{Ic}, MPa m$^{0.5}$	2.5–2.8	3.1–3.4	2.8–3.2
Flexural strength, MPa	400–430	380–400	350–400
Young's modulus, GPa	420–460	400–420	400–420
Sonic velocity, km s^{-1}	13.2–13.8	12.5–13.2	11.5–11.8
Brittleness, $B \times 10^{-6}$, m^{-1}	1230–1770	760–1030	840–1210
Ballistic energy dissipation criterion, $D \times 10^{-12}$, s^{-1} (average)	7.3	4.1	4.4

[a] Water absorption is not greater than 0.02%.

phase (Tables 5 and 6). Regarding RBSC and RBBC ceramics, completeness of the formation of β-SiC and quantity of residual silicon are very important factors, which define the properties of the bonding phase. Properties of conventional RBSC ceramics, such as hardness (Vickers and Knoop) and fracture toughness, are generally higher than of biomorphic RBSC (Table 5) if they are measured for the major SiC or B_4C phase, because larger-size originally introduced SiC or B_4C grains can withstand the action of the sharp indenter better than the "mix" of β-SiC and residual silicon. A higher content of residual silicon for biomorphic RBSC also may be a factor of the lower Young's modulus and stiffness (defined as Young's modulus/density) comparing with conventional RBSC. However, the comparison of the hardness measurement for the major phase (major grains) and the bonding phase of conventional RBSC shows that the bonding phase (silicon with some amount of β-SiC) has significantly lower properties. Properties of the bonding phase of biomorphic RBSC could not be determined due to more homogeneous structure of this ceramics. Properties of conventional RBSC ceramics produced by different companies have some notable difference, and it is dealt with the difference of the used technologies and starting materials that affect the compaction of the major grains and a content and distribution of residual silicon. For example, for some materials, Vickers and Knoop hardness of the bonding phase could be measured even at 1 kg load, but for some other materials hardness could be tested only at 0.5 kg (or even lower) while extensive cracking occurred at 1-kg loading (it was observed under microscope). Such the difference may be the real factor affecting ballistic performance. It has to be noted that a wide spread of hardness data up to a few hundred kg mm^{-2} (between individual measurements) were observed for all the materials obtained from different ceramic producers because it was not easy to conduct measuring for the single phase. Because of this, hardness values for RBBC ceramics are even lower than for RBSC (it was not possible to measure hardness for the major phase for this ceramics accurately due to the microstructure features). Indentation at 2-kg load (both Knoop and Vickers) was not valid for all these materials due to intensive shattering of the samples under this load. All the

Table 5
Properties of the studied reaction-bonded carbide ceramics.

Property	"Conventional" RBSC[a]	Biomorphic RBSC	"Conventional" RBBC
Density, g cm^{-3}	3.0–3.07	2.8	2.5–2.55
Rockwell hardness *HRA*	90–91	90	90–92
Knoop hardness, kg mm^{-2}			
HK1 (major phase)	2000–2150	1650[b]	1550–1750[b]
HK0.5 (matrix)	1250–1450		
Vickers hardness, kg mm^{-2}			
HV1 (major phase)	2350–2450	2050[b]	1750–1900[b]
HV0.5 (matrix)	1350–1500		
Fracture toughness, K_{Ic}, MPa m$^{0.5}$	2.2–2.8	2.3	2.65
Sonic velocity, km s^{-1}	10.3–11.6	10.4	11.8
Young's modulus, GPa	300–400	290	300–350
Flexural strength, MPa	190–250	180	180–200

[a] The data accumulated for different RBSC ceramics from several different manufacturers.

[b] Average values; the separate testing for the major grains and for the matrix could not be conducted.

Table 6
Properties of the studied SiC-based heterogeneous ceramics.

Property	Ceramics AS-ASN based on starting system SiC–(Si_3N_4)–Al_2O_3	Ceramics ESS-ESAS based on starting system SiC–Si_3N_4–Al_2O_3–Si
Density, g cm^{-3}	2.7–3.2	2.85–3.05
Rockwell hardness		
HRC	40–55	45–55
HRA	58–77	68–78
Flexural strength, MPa	105–155	120–140
Impact strength, kJ m^{-2}	1.86–2.24	–
Young's modulus, GPa	240–310	260–280
Sonic velocity, km s^{-1}	9.8–11.2	9.8–10.05

reaction-bonded ceramics have high Rockwell hardness at high 150-kg load (values of 90 or even greater).

Regarding studied heterogeneous materials prepared without siliconization process, one of the major factors affecting the properties is the heat treatment (firing) conditions, including the firing environment, at which this treatment occurred because they define the composition of the bonding phase. Due to larger sizes of SiC grains (actually, special particle size distributions have been selected for each type of the ceramics), these materials do not have a high level of mechanical properties. The presence of Si_3N_4 and optimized content of Al_2O_3 in the compositions provide the mechanical properties increase (Table 6). Due to clear heterogeneous structure, Rockwell hardness testing is the most applicable for the hardness characterization of these ceramics; this testing method is also well suitable for RBSC and RBBC materials.

Because of heterogeneous structures with significant difference in properties of the phases in the reaction-bonded ceramics and the SiC–(Si_3N_4)–Al_2O_3 ceramics, it is not possible to calculate brittleness and ballistic energy dissipation criterion for these materials.

3.3. Ballistic performance of studied armour ceramics

Ballistic performance of ceramic materials depends on a number of properties. They include density and porosity, hardness, fracture toughness, Young's modulus, sonic velocity, mechanical strength, and some others. Any single property does not have a direct correlation with ballistic performance because the fracture mechanism during the actual bullet impact is very complicated, the crack formation is caused by different stress factors, and it occurs in extremely short time. In short, the microstructural features affecting physical and ballistic properties strongly influence crack propagation and energy dissipation mechanisms and ultimately ballistic performance. Thus, the ceramic structures formed by the grains with different but specially selected sizes or formed by two or more crystalline phases positively affect ballistic performance, but the increase of mechanical properties may not be observed. Hence, all relevant properties, as well as ceramic microstructural features, must be carefully considered in assessments of ballistic performance of protective systems. For instance, ceramics should have high-hardness values in order to defeat a projectile and to decrease its velocity, but the crack propagation in ceramics after impact should not be intensive. In many cases, it is not easy to maintain these both conditions. It is known and confirmed experimentally [16] that some ceramic materials cannot resist high indentation loads, e.g. dense B_4C and SiC ceramics are intensively shattered under the loads greater than 1–2 kg (Vickers or Knoop indentation testing), while some other materials, e.g. alumina, alumina–zirconia, silicon nitride ceramics, can be loaded to 10–20 kg, and their indentation replica is very clear. It is, therefore, difficult to formulate properties requirements for all types of armour ceramics due to their significant difference of fracturing and energy dissipation during ballistic impact. It is more realistic to propose these requirements for each major group of armour ceramics.

Some properties requirements for alumina ceramics, dense homogeneous carbide-based ceramics, heterogeneous RBSC and some other ceramics were discussed in the related studies [4,9,10,12–14]. A semi-phenomenological criterion of evaluation of ballistic energy dissipation ability may be expressed by the formula: $D = 0.36(HV \cdot c \cdot E/K_{Ic}^2)$ [8], which demonstrates that a combination of physical properties of armour ceramics should be considered in their evaluation and selection. Taking into consideration the formula of brittleness $B = HV \cdot E/K_{Ic}^2$, the criterion of ballistic energy dissipation ability may be expressed as $D = 0.36(B \cdot c)$, i.e. brittleness factor may be considered as one of the key factors affecting ballistic performance. However, since ballistic energy dissipation also depends on phase composition and structure of ceramics, the D-factor may be expressed as $D = B \cdot c \cdot S$ (S – "structural" factor) [16]. Comparing studied alumina and alumina–mullite ceramics, they have the same level of brittleness and ballistic energy dissipation ability despite the relatively higher individual physical properties of alumina ceramics. These formulae may be successfully applicable for dense homogeneous armour ceramics. Considering dense armour ceramics with different brittleness B, the materials with higher B values (e.g. carbide-based ceramics) do not perform well in multiple-hit ballistic situations due to increased shattering even after the first ballistic impact. These materials also demonstrate elevated cracking at the higher load hardness testing [16]. For heterogeneous armour ceramics, such as RBSC, RBBS and SiC-based materials AS, ASN, ESAS, ballistic energy dissipation ability and ballistic performance depend, to a significant degree, on phase composition and structure of the ceramics and related crack propagation. For example, the "structural" factor is defined by the content and distribution of residual silicon and grain size of the major SiC phase for conventional and biomorphic RBSC, particle size distribution (i.e. grain compaction) and a content of aluminosilicate or sialon bonding phase in the materials AS, ASN, ESAS.

All the developed or selected for the study ceramics demonstrated a high level of ballistic performance. Armour systems based on the developed alumina, alumina–zirconia and alumina–mullite ceramics bonded with appropriate aramid-based and polyethylene backing materials are capable of

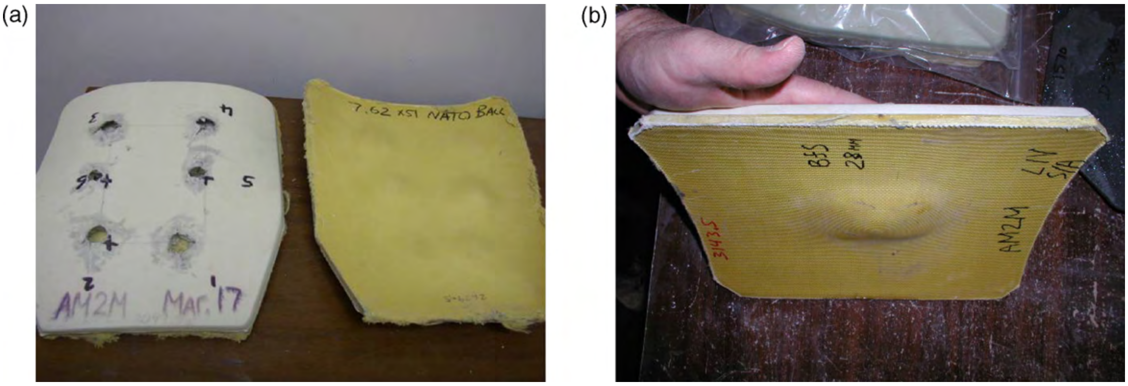

Fig. 5. Ballistic performance of alumina–mullite ceramics AM2. (a) 7.62 × 51 mm NATO Ball FMJ (6 rounds to one plate, no penetration); (b) 7.62 × 63 mm AP M2 (1 round, no penetration).

defeating all threats, which were used for the testing, such as 5.56 × 45 mm SS109, 7.62 × 39 mm Russian and 7.62 × 51 mm NATO Ball FMJ, 7.62 × 54R LPS and others and even 0.308 Lapua and 7.62 × 63 mm AP M2 ammunitions with high kinetic energy. They provided ballistic protection to NIJ Level III or Level IV depending on the type of ceramics and backing materials (e.g. Level IV in conjunction with a ballistic Kevlar^{TM} vest or ‘‘stand alone’’, i.e. without vest). Armour systems based on the mentioned oxide ceramics for personnel protection have satisfactory multi-hit performance (up to 6–7 impacts to one body-armour plate or multiple impacts for large monolithic panels for vehicular ballistic protection). Depending on the ammunition, each material has its own features of fracturing connected with its physical properties and microstructure. Trauma for personnel armour plates made from these materials occurred at acceptable levels (i.e. not greater than 44 mm deformation in accordance with NIJ Standards).

Alumina ceramics with higher hardness demonstrated less trauma and bullet intrusion. However, in this case, a greater degree of a crack growth is observed, probably due to lower brittleness values. Based on the fractography studies and comparing ballistic performance of the considered high-alumina ceramics, the materials, such as AL98 and AL98.5, provide less crack growth but larger trauma than AL99.7; however, they are better for multi-hit performance due to greater energy dissipation ability. At the same time, the ceramics AL99.7 and AL98.5 are more superior for the armour piercing (7.62 × 63 mm AP M2); they could demonstrate successful ballistic performance against two AP rounds to the armour plate with acceptable weights and thickness suitable for body-armour applications. The ceramic AL98.5 may be selected as very acceptable for all types of ballistic situations when multi-hit performance and armour piercing are considered due to the optimal microstructure and mechanical properties. It has to be noted that some alumina ceramics obtained from other manufacturers with similar Al_2O_3 contents, as the developed and considered here, demonstrate elevated cracking, fragmentation and trauma and, therefore, are less reliable and require a thicker backing. This is the evidence that the Al_2O_3 content is not the major factor for the selection of the proper armour material, but microstructure and physical properties dealt with ceramic composition, appropriate grades of starting alumina powders and optimized technology define the required ballistic performance. In the case of AZ ceramics, the cracks are rather short, and trauma is comparable with AL99.7 material. High ballistic performance of AM2 ceramics (see Fig. 5a and b), despite their lower level of mechanical properties, may be explained by high energy dissipation ability (low values of the *D*-criterion) and lower brittleness provided by a presence of two major crystalline phases (corundum and mullite). Probably, the presence of two major phases with relatively high mechanical properties promotes dwelling of the projectiles. This ceramic successfully performs even in the case of armour piercing applications (Fig. 5b). As mentioned above, the penetrator is distorted and eroded during the initial contact with the ceramic and the erosion of the penetrator is greater as the hardness of the ceramic increases. As predicted, the highest level of bullet erosion was observed for the hardest ceramics, such as AZ and AL99.7 ceramics, which correlates well with the data [7]. These materials perform better against armour piercing projectiles with the highest hardness and kinetic energy, such as with a WC core; however, as mentioned above, AZ ceramics has a limited application due to its higher density and weight.

Different kinds of cracks are formed during the ballistic impact (Fig. 6). A locus of conoidal coaxial cracks starts at the impact point; while radial tensile cracks are initiated at the back surface close to the axis of impact. Star cracks are formed at the side of conoids. Tangential spall cracks occur due to shear stress waves reflected from the edges of a plate and due to the formation of the cone cracks; lateral spall cracks may also form due to the longitudinal stress waves reflected from the backing support. Fragments of damaged ceramics with different sizes ranging from big chunks to a fine powder are observed after fracturing. This observation is inherent to dense alumina, alumina–zirconia and alumina–mullite ceramics with lower brittleness. Comparing the studied materials, less powdering was observed for AZ ceramics.

Analyzing microstructure, properties and crack formation of dense homogeneous ceramics based on Al_2O_3, it can be noted that cracks propagate in a higher extent if the ceramics have some defects related to manufacturing issues (e.g. micro-voids or flaws, or if the material has less homogeneity related to less uniform distribution of the glassy phase). This analysis was

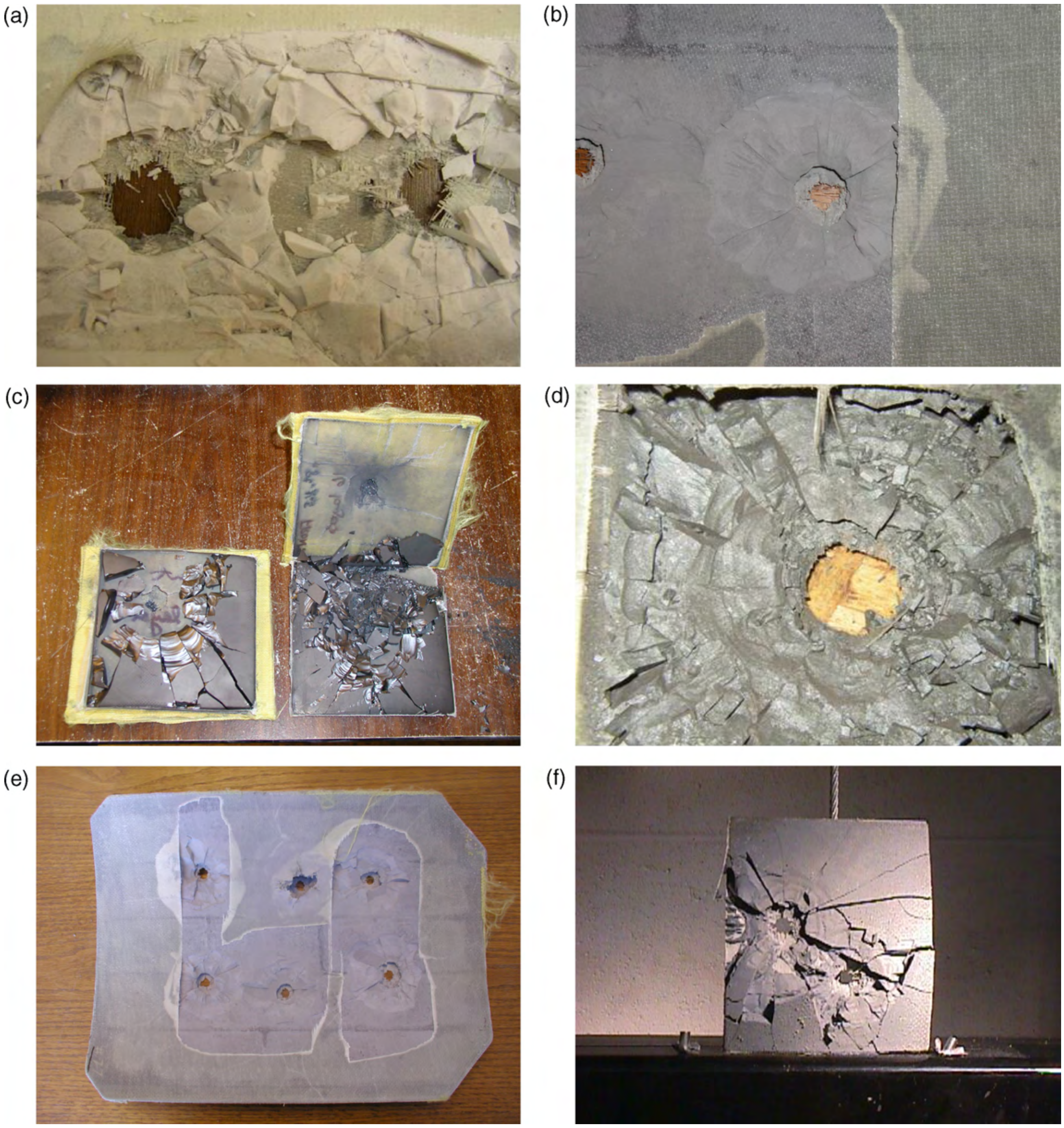

Fig. 6. Fracturing of ceramics after ballistic impact. (a) AM2 ceramics, 7.62 × 63 mm AP M2 (some fragments were removed); (b) RBSC ceramics, 7.62 × 54R LPS; (c) dense SiC ceramics, 7.62 × 51 mm NATO Ball FMJ; (d) biomorphic RBSC, 7.62 × 63 mm AP M2; (e) ASN ceramics, 7.62 × 51 mm NATO Ball FMJ; (f) AS ceramics, 7.62 × 51 mm NATO Ball FMJ, 2 rounds to 1 tile (110 × 110 mm).

done not only for the developed ceramics (in order to minimize the influence of the manufacturing issues affecting homogeneity of microstructure and properties, special process improvement actions have been implemented), but also for alumina ceramics with similar compositions obtained from some other manufacturers. This data are well correlated to the general concept related to the influence of lower homogeneity and the presence of micro-defects on crack formation and breakage of advanced ceramics, and they also are confirmed by the hardness measuring (microstructure studies under indentation).

Studied heterogeneous SiC-based ceramics also demonstrated high ballistic performance. Armour systems based on these ceramics are capable of defeating 5.56 × 45 mm SS109, 7.62 × 39 mm and 7.62 × 51 mm NATO Ball FMJ and 7.62 × 54R LPS ammunitions providing ballistic protection to NIJ Level III with high multi-hit performance (up to 6 hits to one plate) (see examples on Fig. 7a and b). Ballistic test results also confirmed the importance of microstructure and ballistic impact energy dissipation ability of ceramics on ballistic performance. During ballistic impact, the SiC grains promote ‘‘stopping’’ a high-velocity projectile by decrease significantly the projectile velocity. The crystalline–glassy bonding phase is fractured, but the propagated cracks are stopped at the hard SiC grains surface or on the pore surface. The Si_3N_4- and SiAlON-containing bonding phases promote the reduction of the crack propagation. In the case of RBSC and RBBC ceramics, the fracturing occurs through residual silicon as the weakest and the most brittle phase. The damage zone is characterized by large and small chunks and powder (Fig. 6b). However, the balance

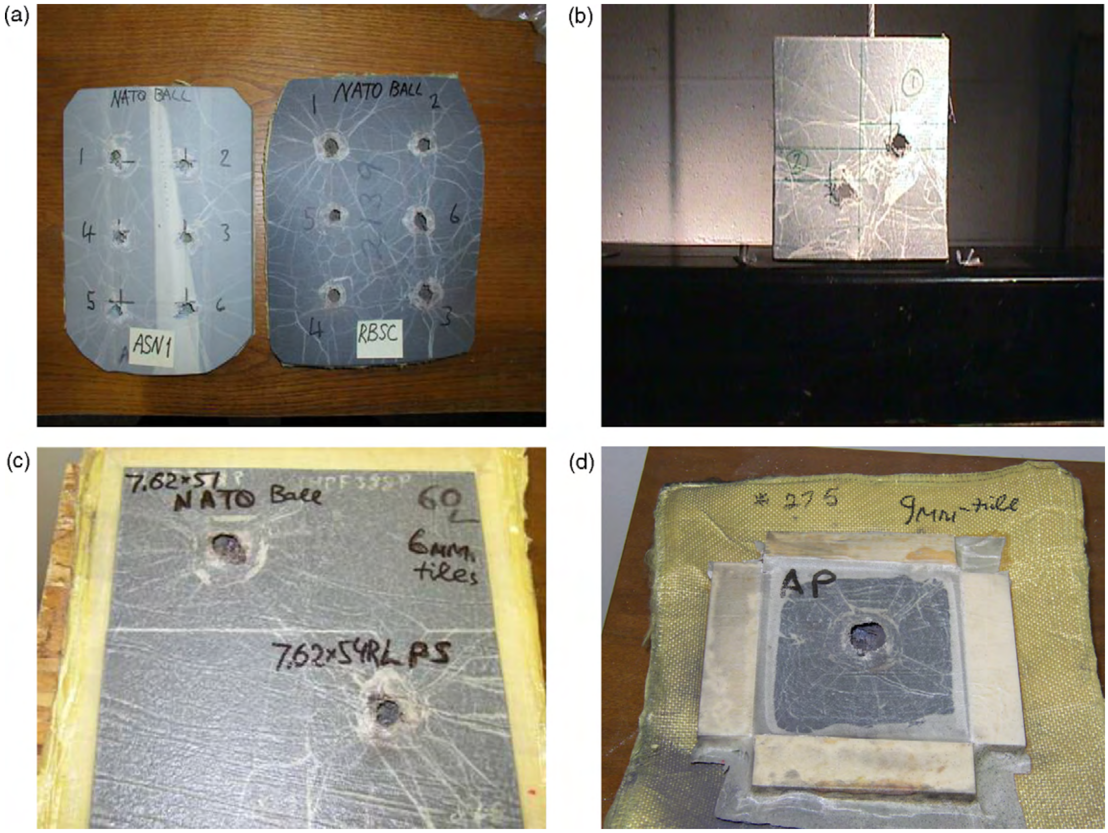

Fig. 7. Ballistic test results for heterogeneous SiC-based ceramics. (a) ASN and RBSC ceramics (body-armour plates), 7.62 × 51 mm NATO Ball FMJ; (b) AS ceramics, 7.62 × 51 mm NATO Ball FMJ 2 rounds to one tile (110 × 110 mm); (c) biomorphic RBSC, 7.62 × 51 mm NATO Ball FMJ (top) and 7.62 × 54R LPS (bottom); (d) biomorphic RBSC (tile 100 × 100 mm), 7.62 × 63 mm AP M2.

of the ceramic plate is relatively intact, and it can provide further ballistic protection relatively close to the initial impact. The damage zone has a ‘‘traditional’’ conical shape with a locus of conoidal cracks initiated at the impact point and radial cracks initiated at the back surface. Some other kinds of cracks also may be observed. However, the presence of spall cracks is minimal, and special spall protection is not required for the materials such as AS and ASN. The bonding phase composition may have a key role in fracturing and ballistic performance. For example, if the bonding matrix in RBSC or RBBC ceramics has lower hardness, i.e. if the level of ‘‘bonding’’ is not high enough (it may happen either in the case of a lower content of the formed β-SiC or in the case of an excessive content of residual Si), the ceramics have elevated fracturing and elongated cracks upon ballistic impacts and, as a result, lower ballistic performance, especially in the case of multi-hit situations. The weakening of RBSC ceramics related with the presence of residual Si is dealt with the Si transformation under ballistic impact (phase transformation of Si under mechanical loads was noted by Domnich and Gogotsi [18]). Manufacturing defects (flaws, microcracks, etc.) increase crack propagation. However, with appropriate armour system design, i.e. with right selection of thickness of ceramics and type and thickness of backing, the materials can withstand even armour piercing rounds (see Fig. 6d demonstrating performance of biomorphic RBSC ceramics).

Dense hot-pressed and pressureless sintered B_4C and SiC ceramics with microcrystalline structures demonstrated another type of fracturing than alumina, alumina–mullite or heterogeneous SiC-based ceramics. Despite high hardness (at low indentation loads) and other mechanical properties, the mentioned homogeneous carbide ceramics demonstrated intensive shattering, complete disintegration of the impact zone and intensive crack propagation (Fig. 6c). Intergranular cleavage may be expected at the ballistic impact because it was observed at the hardness testing at elevated loads. ‘‘Powdering’’ at the impact zone is well observed. Hot-pressed carbide ceramics perform better than pressureless sintered due to better densification and higher related mechanical properties. Although they can defeat 5.56 × 45 mm, NATO Ball, LPS and AP ammunitions, these homogeneous carbide materials are not well suited to multi-hit applications (large size body-armour plates with a thickness of the ceramics as 5–9 mm can stop only three rounds). After the first rounds, the disintegrated zone cannot support the adjacent area of the ceramic plate because of intensive shattering and ‘‘powdering’’. Opposite to dense hot-pressed and pressureless sintered carbide ceramics, alumina, alumina–mullite and heterogeneous SiC-based ceramics with the same thickness can withstand up to 6–8 rounds (depending of the thickness of ceramic and backing components) because the large fragments of these ceramics, even after impacts, can support the adjacent area of the armour (Figs. 6e and 7a). Lower

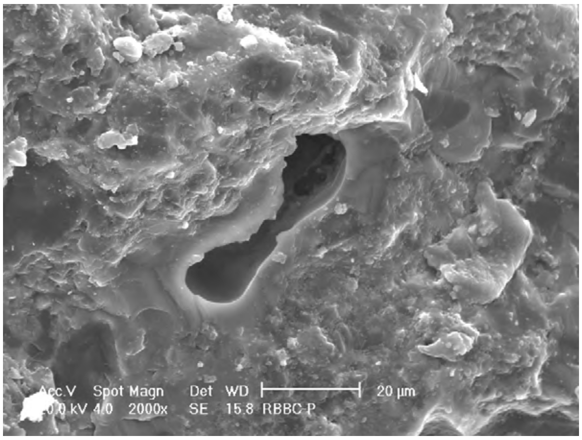

Fig. 8. RBBC ceramics with structural defect (this defect may be a cause of decrease of ballistic performance).

than expected ballistic performance of dense B_4C and SiC ceramics, especially at the AP shooting conditions, also dealt with a local amorphization or phase transformation of the major phases under mechanical loads and ballistic impact [18,19].

Similar negative influence of the presence of micro-defects on crack propagation (as for dense Al_2O_3-based materials) can be noted for dense carbide ceramics, as well as RBBC and RBSC (Fig. 8). Additionally, the presence of the small carbonaceous inclusions and their amounts and distribution in the ceramics dealt with the quality of starting carbide materials and infiltration process and incompleteness of reaction bonding for RBSC or RBBC ceramics may be important factors affecting fracturing and decrease of ballistic performance, especially under the action of harder projectiles. This is confirmed by the hardness measuring (microstructure studies of the indentations), i.e. the cracks are originated and propagated easier under indentations from the soft carbonaceous inclusions, flaws and other micro-defects.

In general, a projectile energy is decreased by approximately three times within 20 μs of projectile impact [1], and the rate of the loss of energy and, therefore, ballistic performance, depend on the loss of a projectile mass and the loss of a projectile velocity. The loss of a projectile mass occurs when the projectile is defeated by high-hardness ceramics and is eroded due to a high-friction effect. The coarse SiC grains with a size of 50–120 μm used in the studied ceramic compositions have a great abrasiveness, and they erode the moving projectile significantly. For example, projectiles such as 7.62 × 51 mm NATO Ball FMJ and 7.62 × 54R LPS after ballistic impacts on the studied heterogeneous SiC-based ceramics had high damage and erosion that is especially observed in the case of the $SiC–Al_2O_3–Si_3N_4$-based ceramics with a high percentage of coarse SiC grains in the composition. It is difficult to evaluate the decrease of projectile velocity when it moves through a ceramic armor system. However, it may be postulated that high-abrasive large-sized particles, such as the SiC grains, promote remarkable friction between these grains and the moving projectile and, hence, may promote the decrease of a projectile velocity more efficiently than the fine-sized particles used for pressureless sintered ceramics. Characteristics of fracturing and crack propagation for these types of SiC-based ceramics (AS, ASN, ESAS) are similar to RBSC ceramics, and they distinguish from hot-pressed or pressureless sintered dense microcrystalline B_4C and SiC armour ceramics. However, the studied heterogeneous SiC-based ceramics, even RBSC ceramics, are not as superior against AP projectiles with a WC core as the studied alumina, alumina–zirconia and alumina–mullite ceramics, as well as hot-pressed B_4C ceramics. Comparing fracturing of biomorphic and conventional RBSC materials after ballistic impacts, biomorphic materials demonstrate more ‘‘powdering’’, although not as high extent as homogeneous dense carbide-based materials. This elevated powdering for biomorphic RBSC in comparison with conventional RBSC may be explained by a higher content of residual Si and significantly finer grains of the major SiC phase.

4. Conclusion

Ballistic performance of different ceramic armour materials, such as homogeneous high-alumina ceramics and lower-weight alumina–mullite ceramics, homogeneous dense silicon carbide and boron carbide ceramics (pressureless sintered and hot-pressed), heterogeneous reaction-bonded carbide ceramics, including biomorphic ceramics, and heterogeneous silicon carbide-based ceramics developed in the systems, such as $SiC–Al_2O_3$, $SiC–Si_3N_4–Al_2O_3$, mostly obtained through the development, was reviewed. The performance was considered based on structure and properties of the ceramics, as well as the features of armour system designs. Only a combination of all relevant physical properties and microstructure, including the ability to dissipate ballistic energy, as well as optimization of manufacturing processes, should be considered for proper selection and evaluation of ceramic armour. It has been demonstrated that not only dense homogeneous advanced ceramics, but also heterogeneous materials with optimal compositions and structures, have remarkable ballistic performance. It was shown that lightweight inexpensive armour systems with multi-hit performance can be obtained utilizing properties of the ceramic armour materials and their features of fracturing under ballistic impacts. It is not possible to recommend the ‘‘best’’ ceramic material that may be the most suitable for each ballistic situation also taking into account the manufacturing ability, weight and cost. Opposite, the appropriate material can be selected based on particular situation and ballistic requirements.

Acknowledgements

The author is grateful to the specialists from Ceramic Protection Corporation (Calgary, AB, Canada), with whom the author worked for a long period of time, for the assistance in the studies, ballistic testing and discussions of the results. Also the assistance of Alberta Research Council (Edmonton, AB, Canada) in some ceramic properties testing, e.g. hardness and fracture toughness, is appreciated.

References

[1] C.F. Cline, M.L. Wilkins, The importance of material properties in ceramic armor, in: DCIC Report 69-1; Part I: Ceramic Armor, 1969, pp. 13–18.

[2] R.L. Landingham, A.W. Casey, Final Report of the Light Armor Materials Program, UCRL-57269, 1972.

[3] S.-K. Chung, Fracture characterization of armor ceramics, Am. Ceram. Soc. Bull. 69 (3) (1990) 358–366.

[4] D.J. Viechnicki, M.J. Slavin, M.I. Kliman, Development and current status of armor ceramics, Am. Ceram. Soc. Bull. 70 (6) (1991) 1035–1039.

[5] I.Yu. Kelina, Yu.I. Dobrinskii, Efficiency of the use of silicon nitride ceramics as an armor material, Refract. Tech. Ceram. 6 (1997) 9–12 (in Russian).

[6] B. Matchen, Application of ceramics in armor products; key engineering materials, in: H. Mostaghasi (Ed.), Advanced Ceramic Materials, vols. 122–124, Trans. Tech. Publications, Switzerland, 1996, pp. 333–342.

[7] R.G. O'Donnell, An investigation of the fragmentation behaviour of impacted ceramics, J. Mater. Sci. Lett. 10 (1991) 685–688.

[8] V.C. Neshpor, G.P. Zaitsev, E.J. Dovgal, et al., Armour ceramics ballistic efficiency evaluation, in: P. Vincenzini (Ed.), Ceramics: Charting the Future, Proceedings of the 8th CIMTEC, Florence, Italy 28 June–4 July 1994, (1995), pp. 2395–2401, Techna S.r.l..

[9] E. Medvedovski, Alumina ceramics for ballistic protection, Am. Ceram. Soc. Bull. 81 (3) (2002) 27–32;
E. Medvedovski, Alumina ceramics for ballistic protection, Am. Ceram. Soc. Bull. 81 (4) (2002) 45–50.

[10] B. James, Practical issues in ceramic armour design, in: J.W. McCauley, A. Crowson, W.A. Gooch, Jr., et al. (Eds.), Ceramic Armor Materials by Design, Ceramic Transactions, vol. 134, American Ceramic Society, Westerville, OH, 2002, pp. 33–44.

[11] B.A. Galanov, O.N. Grigoriev, S.M. Ivanov, et al., Structure and properties of shock-resistant ceramics developed at the institute for problems in materials science, in: J.W. McCauley, A. Crowson, W.A. Gooch, Jr., et al. (Eds.), Ceramic Armor Materials by Design, Ceramic Transactions, vol. 134, American Ceramic Society, Westerville, OH, 2002 , pp. 73–81.

[12] E. Medvedovski, Alumina–mullite ceramics for structural applications, Ceram. Int. 32 (2006) 369–375.

[13] M.K. Aghajanian, B.N. Morgan, J.R. Singh, et al., A new family of reaction bonded ceramics for armor applications, in: J.W. McCauley, A. Crowson, W.A. Gooch, Jr., et al. (Eds.), Ceramic Armor Materials by Design, Ceramic Transactions, vol. 134, American Ceramic Society, Westerville, OH, 2002, pp. 527–539.

[14] E. Medvedovski, Silicon carbide-based ceramics for ballistic protection, in: E. Medvedovski (Ed.), Ceramic Armor and Armor Systems, Ceramic Transactions, vol. 151, American Ceramic Society, Westerville, OH, 2003 , pp. 19–35.

[15] B. Heidenreich, M. Gahr, E. Medvedovski, Biomorphic reaction bonded silicon carbide ceramics for armor applications, in: E. Medvedovski (Ed.), Ceramic Armor and Armor Systems II, Ceramic Transactions, vol. 178, American Ceramic Society, Westerville, OH, 2005, pp. 45–53.

[16] E. Medvedovski, P Sarkar, Indentation testing of armor ceramics, in: E. Lara-Curzio, M.J. Readey (Eds.), Ceramic Engineering and Science Proceedings, vol. 25, 2004, pp. 589–596, no. 3.

[17] J.B. Quinn, G.D. Quinn, On the hardness and brittleness of ceramics, Key Engineering Materials, vols. 132–136, Trans Tech Publications, Switzerland, 1997, pp. 460–463.

[18] V. Domnich, Y. Gogotsi, Phase transformation in silicon under contact loading, Rev. Adv. Mater. Sci. 3 (2002) 1–36.

[19] M. Chen, J.W. McCauley, K.J. Hemker, Shock induced localized amorphization in boron carbide, Science 299 (7) (2003) 1563–1566.